

# Nanostructural Analysis of Bright Metal Surfaces in Relation to their Reflectivities

N. D. Nikolić,<sup>1</sup> Z. Rakočević<sup>2</sup> and K. I. Popov<sup>3</sup>

<sup>1</sup>ICTM–Institute of Electrochemistry, Belgrade, Serbia and Montenegro

<sup>2</sup>Vinča Institute of Nuclear Sciences, Belgrade, Serbia and Montenegro

<sup>3</sup>Faculty of Technology and Metallurgy, University of Belgrade, Serbia and Montenegro

## I. INTRODUCTION

Electroplating processes are widely used in many branches of industry, the most important of which are: the automobile industries, building and construction industries and electrical and electronics industries. These processes are often used for decorative purposes.

In order for metal coatings to be used for decorative purposes, it is necessary that their surfaces be smooth and bright. In everyday experience the optical properties of the metals are associated with high reflectivity and low transmission. For this reason, the terms “mirror bright”, “semi bright”, and “high bright” are often used when considering electrodeposited-metal coatings.

However, it is known that there are no precise definitions of these terms. Brightness of a metal surface is usually defined as its reflecting power, measured by the amount of light specularly reflected off the surface, *i.e.*, at an angle equal and opposite to that of the incidence light

*Modern Aspects of Electrochemistry, Number 38*, edited by B. E. Conway *et al.* Kluwer Academic/Plenum Publishers, New York, 2005.

with respect to the normal to the geometrical surface. A more precise definition, not involving the actual reflectivity of the surface, would be the ratio between specularly and diffusely reflected light.<sup>1,2</sup> The ratio of specular to total reflectivity can also be used for an estimation of the brightness of a surface.<sup>3</sup>

Structural details which must be fulfilled in order for light from metal surfaces to be to a high degree specularly reflected have not been systematized yet. One of the reasons for the absence of systematized criteria of these characteristics is, among other things, the lack of an appropriate corresponding technique for the examination of the structure of bright metal surfaces. The technique of scanning electron microscopy (SEM), which is usually used for the examination of the structure of metal coatings,<sup>2,4</sup> gives only the information that bright metal coatings have a smaller grain size than mat coatings obtained from a plating bath in the absence of leveling and brightening agents. Over the last few years, the techniques of scanning tunneling microscopy (STM) and atomic force microscopy (AFM) have proven to be very valuable techniques for the examination of metal deposits.<sup>5,6</sup> The value of these techniques lies in their ability to provide *local* information concerning the metal deposit, which is unsurpassed by any other technique owing to the resolution. These techniques enable a precise analysis of the topography of a metal surface, *i.e.*, examination of the submicro structures of metal surfaces to be made. Also, the digital images obtained by these techniques can easily be analyzed by powerful software packages.

## II. REAL SYSTEMS

The (total) reflected light from an ideally flat (geometrical) surface is exclusively mirror reflected light, *i.e.*, the light is reflected at an angle equal and opposite to that of the incident light with respect to the normal to the geometrical surface. On the other hand, any (every) real surface possesses surface irregularities, which lead to scattering of the light. Then, reflected light from a metal surface includes diffusely reflected, not only specularly reflected light.

According to Bockris and Razumney,<sup>1</sup> if the brightness of a surface is defined as the ability to reflect light only in a direction making an angle with the normal equal to that of the incident beam (*i.e.*, approach to an "ideal mirror"), then the surface will be

increasingly bright as the scattering introduced in the reflected light by surface irregularities decreases, that is, as deviations of the actual surface from the ideal, geometrical boundaries are eliminated.

The system which is the nearest approximation to an ideally flat surface, from which reflection of light is exclusively mirror reflection, is the surface of a silver mirror or of mercury. For that reason, reflection and structural characteristics of a silver mirror surface were firstly examined in order to define the reference standard for the comparison of reflection and structural characteristics of different metal surfaces.<sup>7,8</sup> Silver mirror surface is obtained by chemical deposition of silver onto a glass by the silver mirror reaction.<sup>9</sup>

The opposite case of that of a silver mirror surface are metal coatings obtained from solution without brightening addition agents. These metal surfaces are usually known as mat surfaces.

## 1. Limiting Cases

### (i) *Silver Mirror Surface*

#### (a) *Reflection analysis*

The ideal (theoretical) reflectance of silver<sup>10</sup> and the degrees of total, mirror and diffuse reflection as a function of visible light wavelength for a silver mirror surface are given in Fig. 1. Figure 1 shows clearly that the reflection of light from this surface is mostly mirror reflection and the degree of diffuse reflection is very small (up to 2 %). The degree of mirror reflection from a silver mirror is also very close to the ideal reflectance of silver.

#### (b) *Structural analysis*

The 3D (three-dimensional) STM image (700 x 700) nm of a silver mirror surface is shown in Fig. 2, from which it can be seen that the surface of such a mirror is very smooth.

The line section analysis of this surface is shown in Fig. 3, which indicates that this surface consisted of relatively flat and mutually parallel parts. The STM software measurements showed that distances between adjacent, relatively flat, parts were several atomic diameters of silver.<sup>11</sup>

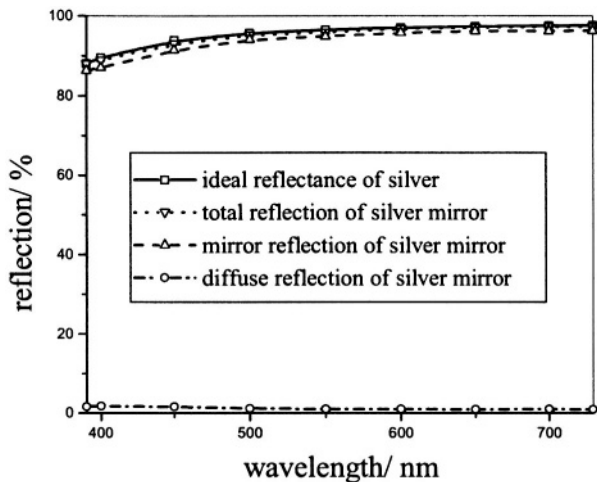


Figure 1. The dependence of the degrees of reflection on the visible light wavelength for the ideal reflectance of silver ( $\square$ ), the total ( $\nabla$ ), mirror ( $\Delta$ ) and diffuse (o) reflections of a silver mirror. (Reprinted from Ref.<sup>7</sup> with permission from the Serbian Chemical Society.)

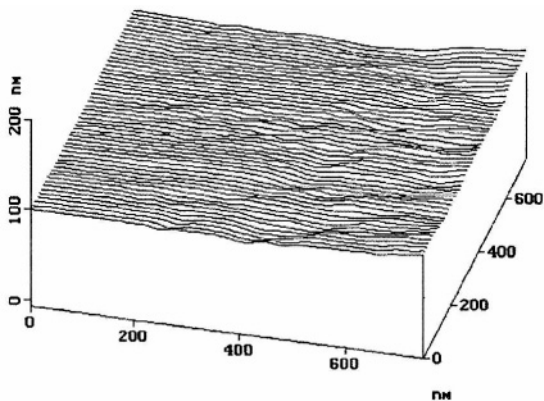


Figure 2. 3D STM image of a silver mirror surface. Scan size: (700 x 700) nm. (Reprinted from Ref.<sup>7</sup> with permission from the Serbian Chemical Society.)

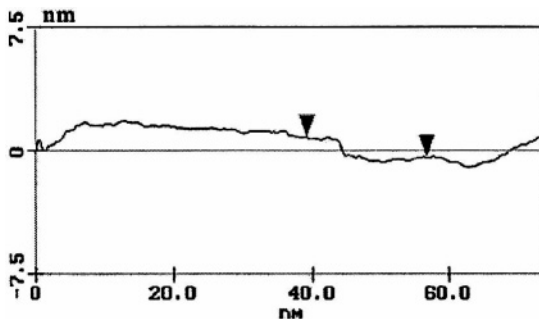


Figure 3. Line section analysis of a portion of the STM surface shown in Fig. 2. The vertical distance between the markers represents 1.246 nm. (Reprinted from Ref. <sup>7</sup> with permission from the Serbian Chemical Society.)

The line section analysis of a relatively flat part of the surface is shown in Fig. 4. It was shown by STM software data processing that the roughness of the flat part of the surface is less than the atomic diameter of silver, *i.e.*, the flat parts are smooth on the atomic scale. The atomic arrangement of a flat part of a surface is shown in Fig. 5.

Finally, the reflection of light from the silver mirror surface is mostly mirror reflection which is very close to the ideal reflectance of silver. The structural characteristics of this surface, which enable a high degree of

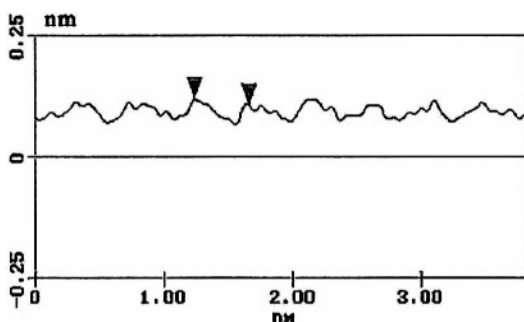


Figure 4. Line section analysis of the flat part of the surface shown in Fig. 3. (Reprinted from Ref. <sup>7</sup> with permission from the Serbian Chemical Society.)

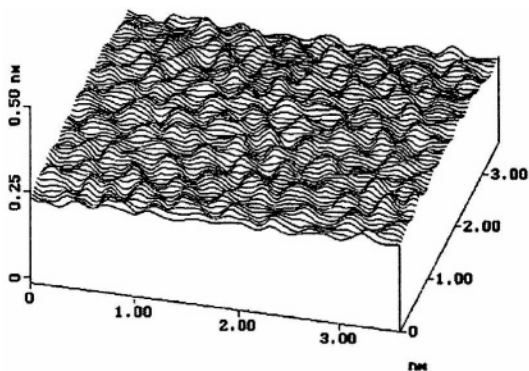


Figure 5. 3D STM image of a silver mirror surface. Scan size: (3.50 x 3.50) nm. (Reprinted from Ref.<sup>7</sup> with permission from the Serbian Chemical Society.)

mirror reflection, are that the surface should have flat and mutually parallel parts which are smooth on the atomic scale, with adjacent flat parts being separated by several atomic diameters of silver.

### (ii) *Mat surfaces*

#### (a) *Reflection analysis*

Figure 6 shows the ideal reflectance of copper<sup>10</sup> and the degrees of total, mirror and diffuse reflection as a function of visible light wavelength for the copper coating obtained from a pure sulfate solution (composition:  $240 \text{ g l}^{-1} \text{ CuSO}_4 \cdot 5 \text{ H}_2\text{O} + 60 \text{ g l}^{-1} \text{ H}_2\text{SO}_4$ ). It can be seen from Fig. 6 that the reflection of light from this coating is mostly of the diffuse kind. The extent of mirror reflection from this coating reaches a maximum of 6 %.

#### (b) *Structural analysis*

It can be seen from Fig. 7 that surface of the copper coating obtained from a pure sulfate solution is relatively rough.

It can be observed from Figs. 8a and 8b that the surface areas of lateral parts of the surface are larger than the surface areas of flat parts of the same surface.

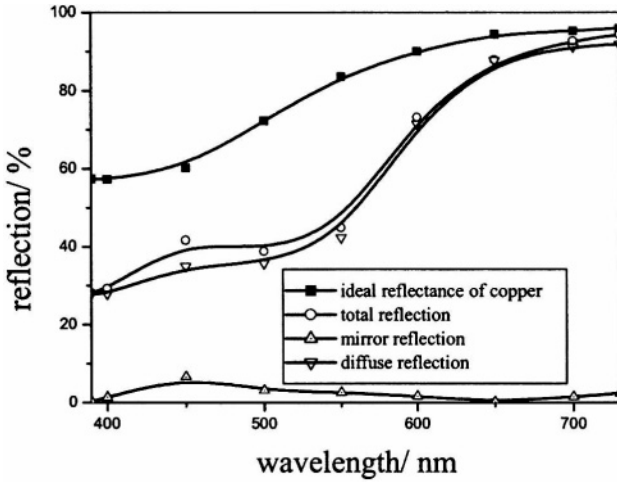


Figure 6. The dependence of the degrees of reflection on the wavelength of visible light for the ideal reflectance of copper (■), the total (○), mirror (Δ) and diffuse (▽) reflections of the copper coating electrodeposited from a pure acid sulfate solution. (Reprinted from Ref.<sup>12</sup> with permission from Elsevier.)

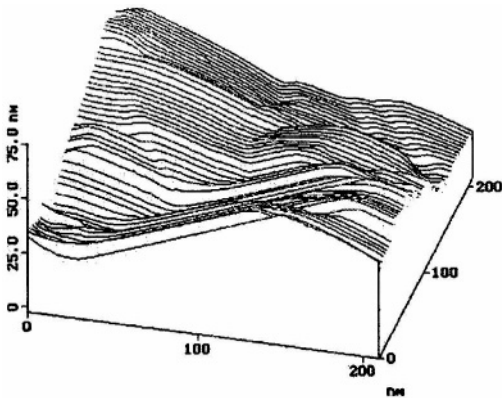


Figure 7. 3D STM image of the copper coating electrodeposited from a pure sulfate solution. (Reprinted from Ref.<sup>13</sup> with permission from Elsevier.)

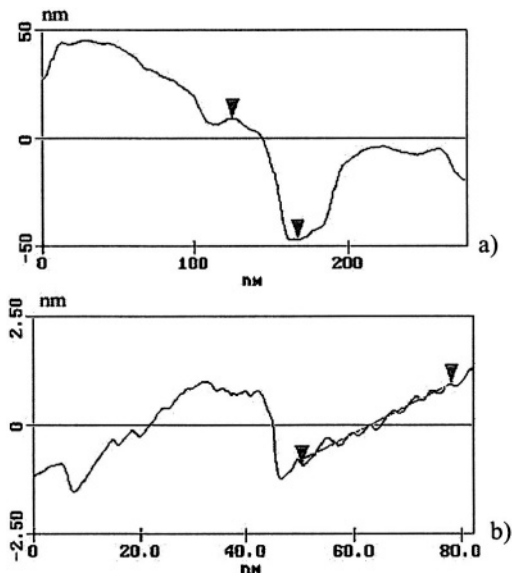


Figure 8. The line section analysis of the copper coating obtained from a pure acid sulfate solution. Scan sizes: a) (300 x 300) nm, b) (80 x 80) nm. (Reprinted from Ref. <sup>12</sup> with permission from Elsevier.)

Finally, the reflection of light from the copper coating obtained from a pure sulfate solution is mostly diffuse reflection. The structural characteristics of this copper surfaces which enabled a high degree of diffuse reflection with a negligible degree of mirror reflection are that the lateral parts of the surface were larger than the flat parts.

## 2. Systems in Metal Finishing

### (i) Polished Copper Surfaces

#### (a) Reflection analysis

The reflection characteristics for the copper surface polished mechanically and the copper surface polished both mechanically and electrochemically<sup>12</sup> are shown in Fig. 9a.



The degrees of mirror and diffuse reflection of the same copper surfaces as a function of wavelength of visible light are shown in Fig. 9b. It can be seen from this figure that electropolishing of the mechanically polished copper surface led to an increase of the degree of mirror reflection and a decrease of the degree of diffuse reflection. The degree of mirror reflection of the copper surface, polished both mechanically and electrochemically, is approximately 15 - 20 % greater than the degree of mirror reflection of the copper surface polished only mechanically, while the degree of diffuse reflection is smaller by 2-10 % than the degree of diffuse reflection of the mechanically polished copper surface. Also, it can be seen from Figs. 9a and 9b that the degrees of mirror reflection of the copper surface, polished both mechanically and electrochemically, approach very nearly the ideal reflectance of copper.

#### *(b) Structural analysis*

Figure 10 shows the copper surface polished mechanically (Fig. 10a) and the copper surface polished both mechanically and electrochemically (Fig. 10b).

Figures 10a and 10b show that the topographies of these copper surfaces differ from one another. Electropolishing of the copper surface, first polished mechanically, led to a decrease of the roughness of this copper surface (Figs. 10a and 10b). Analysis of the topographies of the copper surfaces and the dependences of the degrees of mirror and diffuse reflection as a function of the wavelength of visible light showed that a decrease of the roughness of copper surfaces is accompanied by a decrease of the degree of diffuse reflection and by an increase of the degree of mirror reflection.<sup>12</sup>

It can also be seen from Fig. 10b that the topography of the copper surface, polished both mechanically and electrochemically, consists of small and mutually parallel parts of the surface.

Figure 11 shows the line sections analysis of regions of the copper surfaces shown in Fig. 10. It was shown by the STM data processing that the distance between two flat parts of the copper surface, polished both mechanically and electrochemically, is several atomic diameters of copper.<sup>11</sup> The same distance for the copper surface polished only mechanically is approximately 70 atomic diameters of copper. Also, it can be seen from Figs. 11a and 11b that these relatively flat parts of the surface are to a higher degree mutually parallel for the copper surface

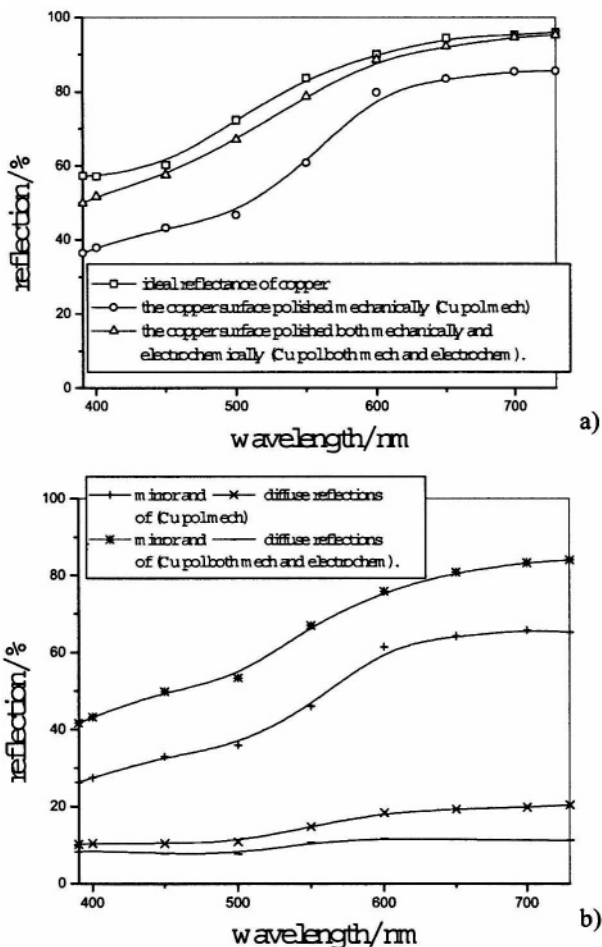


Figure 9. The dependence of the degrees of reflection on the wavelength of visible light for: a) the ideal reflectance of copper ( $n$ ) and the total reflections of the copper surface polished mechanically ( $\circ$ ), the copper surface polished both mechanically and electrochemically ( $\Delta$ ), b) mirror (+) and diffuse (x) reflections of the copper surface polished mechanically; mirror (\*) and diffuse (-) reflections of the copper surface polished both mechanically and electrochemically. (Reprinted from Ref. <sup>12</sup> with permission from Elsevier.)

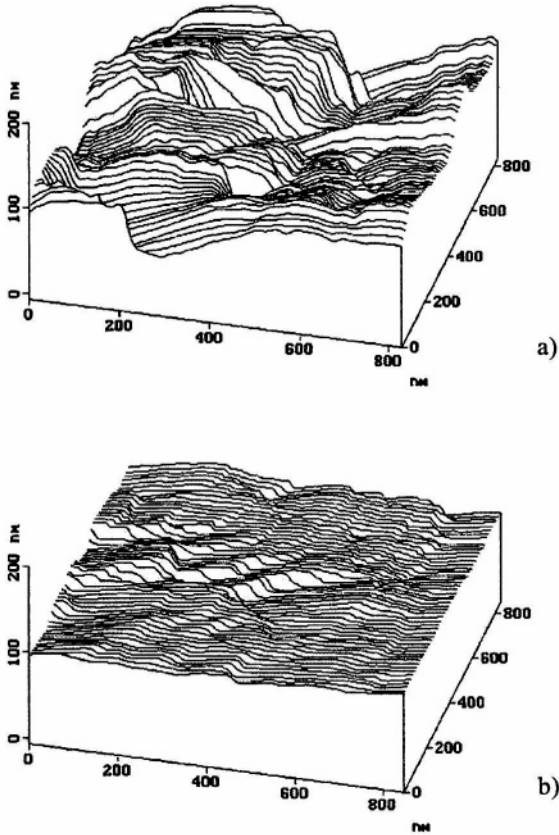


Figure 10. 3D STM images of: a) the copper surface polished mechanically, b) the copper surface polished both mechanically and electrochemically. Scan size: (880 x 880) nm. (Reprinted from Ref.<sup>12</sup> with permission from Elsevier.)

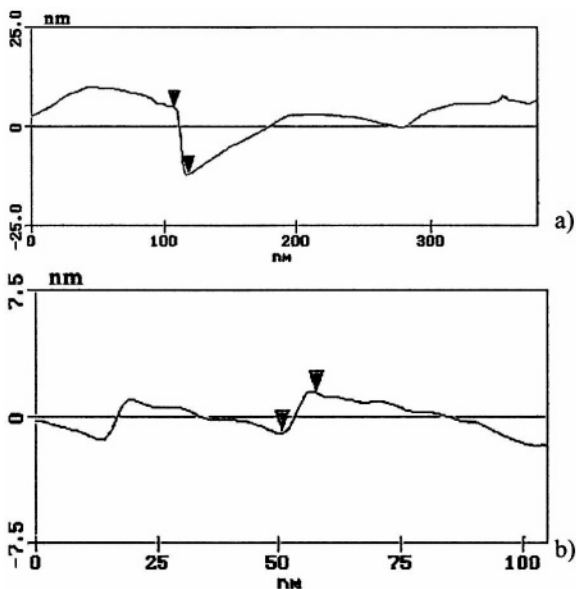


Figure 11. The line sections analysis from the regions of the STM surfaces shown in Fig. 10: a) the copper surface polished mechanically, b) the copper surface polished both mechanically and electrochemically. The vertical distances between markers represent: a) 16.780 nm, b) 2.394 nm. (Reprinted from Ref.<sup>12</sup> with permission from Elsevier.)

polished both mechanically and electrochemically than for the copper surface polished only mechanically.

The line sections analysis of the flat parts of the copper surfaces is shown in Fig. 12. The roughness of the flat parts of the copper surface, polished both mechanically and electrochemically, is very small and less than the atomic diameter of copper. For this reason, it can be said that these flat parts of the surface are smooth on the atomic level. The roughness of the flat parts of the copper surface, only polished mechanically, is less than 2 atomic diameters of copper.<sup>12</sup>

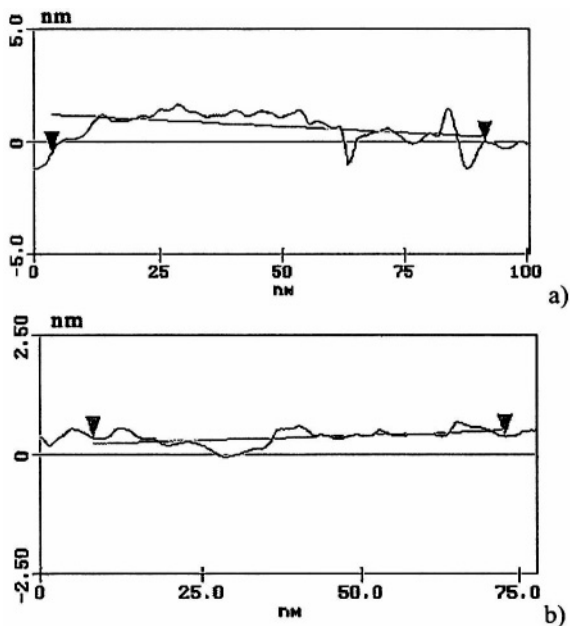


Figure 12. The line sections analysis of the flat parts of surfaces: a) the copper surface polished mechanically, b) the copper surface polished both mechanically and electrochemically. The roughnesses of the observed surfaces were: a) 0.444 nm, b) 0.111. (Reprinted from Ref.<sup>12</sup> with permission from Elsevier.)

The atomic arrangement of a flat part of the copper surface polished both mechanically and electrochemically is shown in Fig. 13.<sup>14</sup>

X-ray diffraction (XRD) analysis of the copper surface, polished both mechanically and electrochemically, is shown in Fig. 14. As can be seen from Fig. 14, a relatively disordered structure of this copper surface arises, with an increased ratio of copper crystallites oriented in (200), (220) and (311) planes.

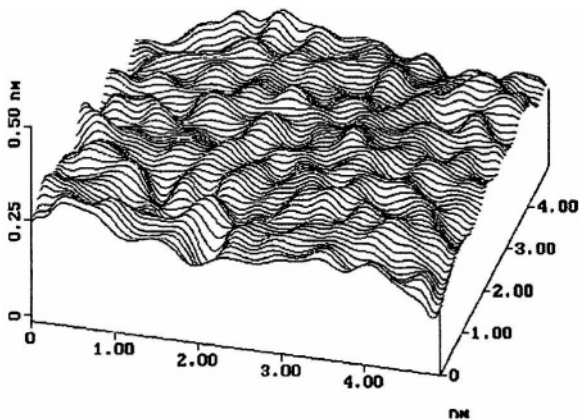


Figure 13. 3D STM image of the copper surface polished both mechanically and electrochemically. Scan size: (5.0 x 5.0) nm. (Reprinted from Ref.<sup>14</sup> with permission from the Serbian Chemical Society.)

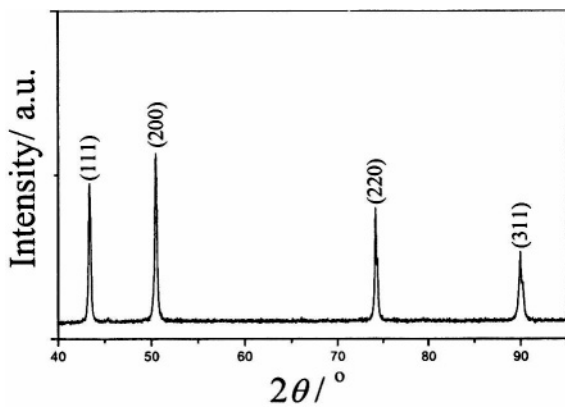


Figure 14. XRD pattern of the copper surface polished both mechanically and electrochemically. (Reprinted from Ref.<sup>12</sup> with permission from Elsevier.)

*(ii) Copper Coatings**(a) Reflection analysis*

The total reflection as a function of the wavelength of light in the visible range for the copper coating obtained in the presence of thiourea (*solution Cu I*:  $240 \text{ g l}^{-1} \text{ CuSO}_4 \cdot 5 \text{ H}_2\text{O} + 60 \text{ g l}^{-1} \text{ H}_2\text{SO}_4 + 0.050 \text{ g l}^{-1}$  thiourea) of  $20 \text{ }\mu\text{m}$  thickness<sup>15</sup> and the copper coating obtained in the presence of modified polyglycol ether (Lutron HF 1), PEG 6000 and 3-mercaptopropane sulfonate (*solution Cu II*:  $240 \text{ g l}^{-1} \text{ CuSO}_4 \cdot 5 \text{ H}_2\text{O} + 60 \text{ g l}^{-1} \text{ H}_2\text{SO}_4 + 0.124 \text{ g l}^{-1} \text{ NaCl} + 1.0 \text{ g l}^{-1}$  modified polyglycol ether (Lutron HF 1) +  $1.0 \text{ g l}^{-1}$  poly(ethylene glycol)  $M_n = 6000$  (PEG 6000) +  $1.5 \text{ mg l}^{-1}$  3-mercaptopropane sulfonate) of the same thickness<sup>15</sup> are shown in Fig. 15a. The degrees of mirror and diffuse reflections of the same copper coatings as a function of wavelength of visible light are shown in Fig. 15b.

Figure 16 shows reflection characteristics of the same copper coatings, but having a  $25 \text{ }\mu\text{m}$  thickness.<sup>12,13</sup>

It can be observed from Figs. 15 and 16 that the reflection characteristics of these copper coatings were very similar to the same characteristics of the copper surface polished both mechanically and electrochemically. Both the copper coatings exhibited high degrees of mirror reflection which approach very nearly the ideal reflectance of copper for the wavelengths above 600 nm. The degrees of diffuse reflection of these copper coatings have approximately the same values.

*(b) Structural analysis*

The 3D STM image of the  $25 \text{ }\mu\text{m}$  thick copper coating obtained from *solution Cu II* is shown in Fig. 17. Figure 18 shows 3D STM images at higher magnification (*i.e.*, smaller scan size) of the copper coating obtained from *solution Cu I* and the copper coating obtained from *solution Cu II*, thicknesses of  $20 \text{ }\mu\text{m}$  (Figs. 18a and 18b, respectively) and  $25 \text{ }\mu\text{m}$  (Figs. 18c and 18d, respectively).

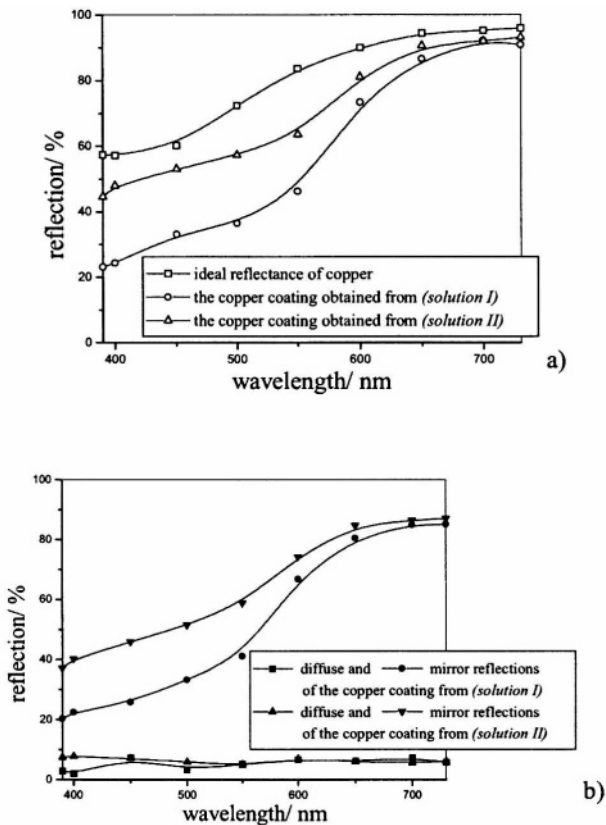


Figure 15. The dependence of the degrees of reflection on the wavelength of visible light for: a) the ideal reflectance of copper (□) and the total reflections of the copper coating electrodeposited from *solution Cu I* (○), the copper coating electrodeposited from *solution Cu II* (△), b) mirror (●) and diffuse (■) reflections of the copper coating electrodeposited from *solution Cu I*, mirror (▼) and diffuse (▲) reflections of the copper coating electrodeposited from *solution Cu II*. (Reprinted from Ref.<sup>15</sup> with permission from Springer-Verlag.)



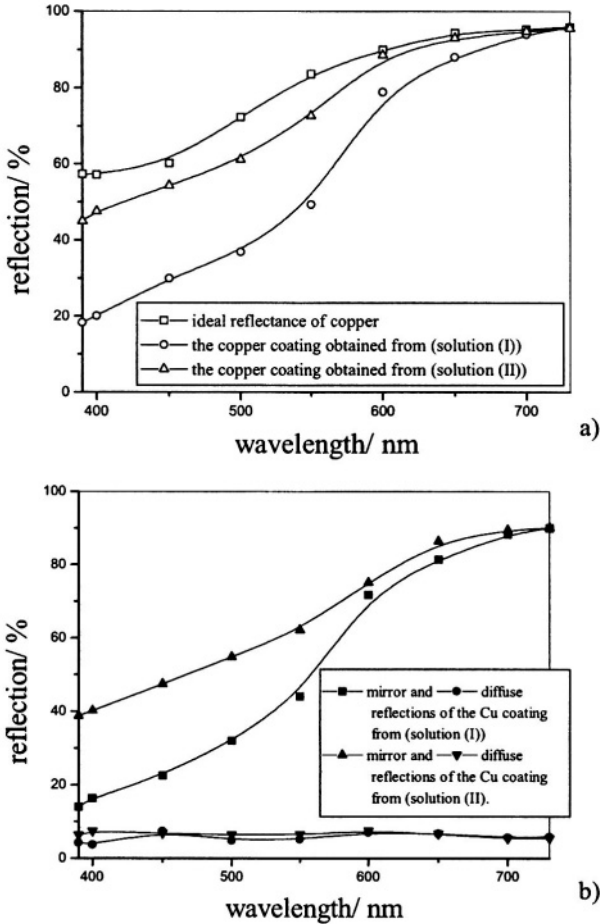


Figure 16. The dependence of the degrees of reflection on the wavelength of visible light for: a) the ideal reflectance of copper (□) and the total reflections of the copper coating electrodeposited from *solution Cu I* (○),<sup>13</sup> the copper coating electrodeposited from *solution Cu II* (△),<sup>12</sup> b) mirror (■) and diffuse (●) reflections of the copper coating electrodeposited from *solution Cu I*,<sup>13</sup> mirror (▲) and diffuse (▼) reflections of the copper coating electrodeposited from *solution Cu II*.<sup>12</sup> (Reprinted from Ref. <sup>12</sup> and Ref. <sup>13</sup> with permission from Elsevier.)

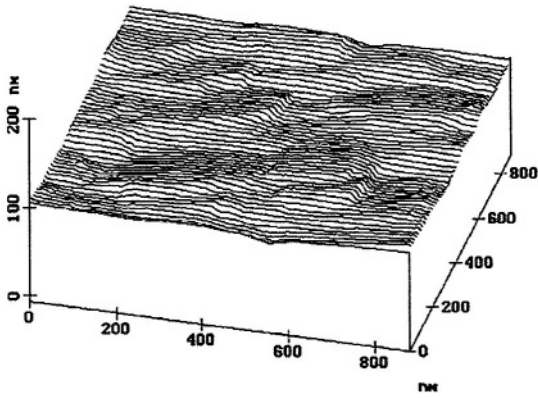


Figure 17. 3D STM image of 25  $\mu\text{m}$  thick the copper coating electrodeposited from *solution Cu II*. Scan size: (880 x 880) nm. (Reprinted from Ref. <sup>12</sup> with permission from Elsevier.)

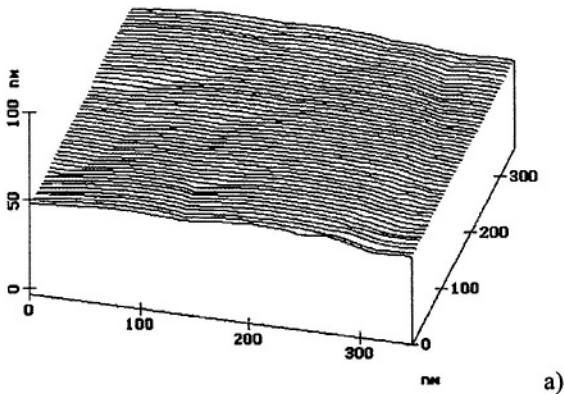


Figure 18. 3 D STM images of copper coatings electrodeposited from: a) *solution Cu I*, thickness of the coating:  $\delta \approx 20 \mu\text{m}$ ,<sup>15</sup> b) *solution Cu II*,  $\delta = 20 \mu\text{m}$ ,<sup>15</sup> c) *solution Cu I*,  $\delta = 25 \mu\text{m}$ ,<sup>13</sup> d) *solution II*,  $\delta = 25 \mu\text{m}$ .<sup>16</sup> (Reprinted from Refs. <sup>13,15,16</sup> with permission from Elsevier, Springer-Verlag and Union of Engineers and Technicians for Protecting of Materials of Serbia, respectively.)

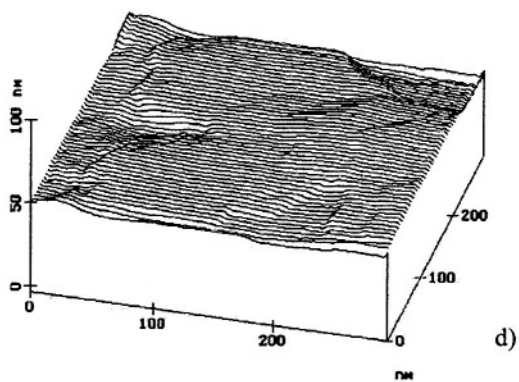
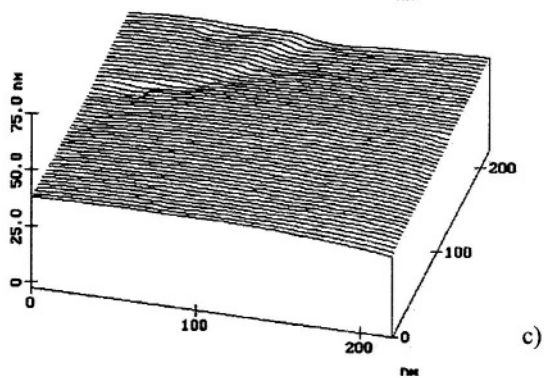
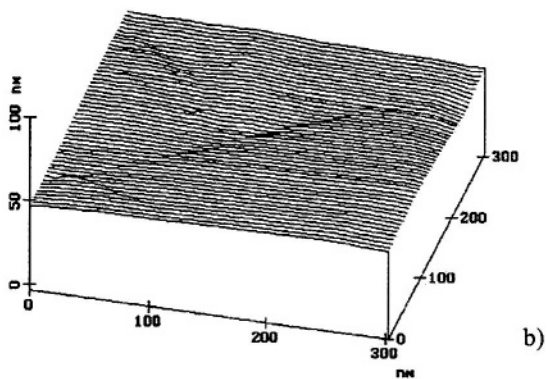


Figure 18. Continuation

Figure 19 shows the line sections analysis of portions of the copper surfaces shown in Fig. 18, while the line sections analysis of the flat parts of these copper surfaces are shown in Fig. 20.

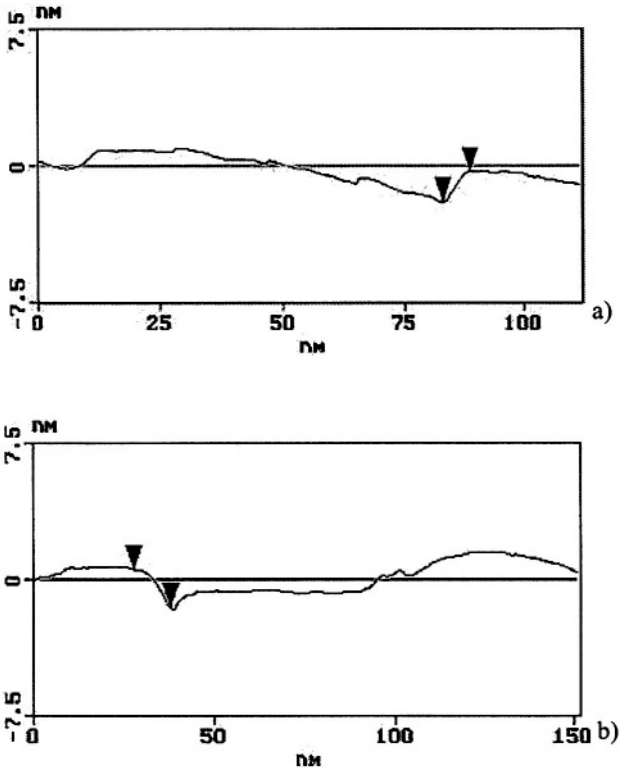


Figure 19. The line sections analysis from the portion of the STM surfaces of the copper coatings shown in Fig. 18 electrodeposited from: a) *solution Cu I*,  $\delta = 20 \mu\text{m}$ ,<sup>15</sup> b) *solution Cu II*,  $\delta = 20 \mu\text{m}$ ,<sup>15</sup> c) *solution Cu I*,  $\delta = 25 \mu\text{m}$ ,<sup>13</sup> d) *solution Cu II*,  $\delta = 25 \mu\text{m}$ .<sup>12</sup> The distances between markers represent: a) 1.656 nm, b) 2.136 nm, c) 1.443 nm, d) 1.177 nm. (Reprinted from Refs.<sup>12,13,15</sup> with permission from Elsevier and Springer-Verlag.)

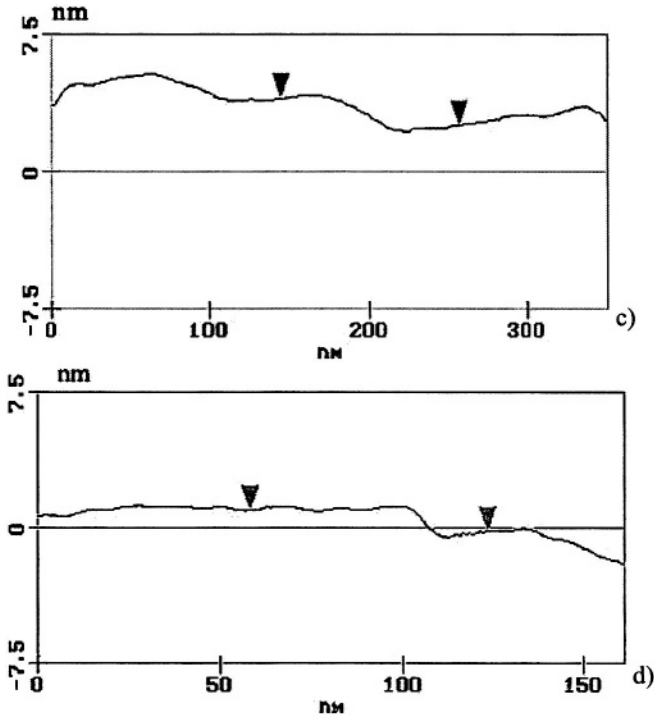


Figure 19. Continuation

Similar reflection and structural characteristics to them showed and  $40 \mu\text{m}$  thick the copper coating obtained from *solution Cu I*. The line section analysis of this copper coating is shown in Fig. 21. The atomically flat parts of these copper coatings are shown in Fig. 22.

The mean size of these atomically flat parts was estimated by STM software measurements, using option of the determination of the autocovariance (ACVF) and power spectral density (PSD) functions. The estimated mean sizes of the flat parts are given in Table 1.

Structural characteristics of the formed copper coatings were very similar to the same characteristics of the copper surface polished both mechanically and electrochemically. The surfaces of these copper coatings consisted of flat and mutually parallel parts of the surface. The

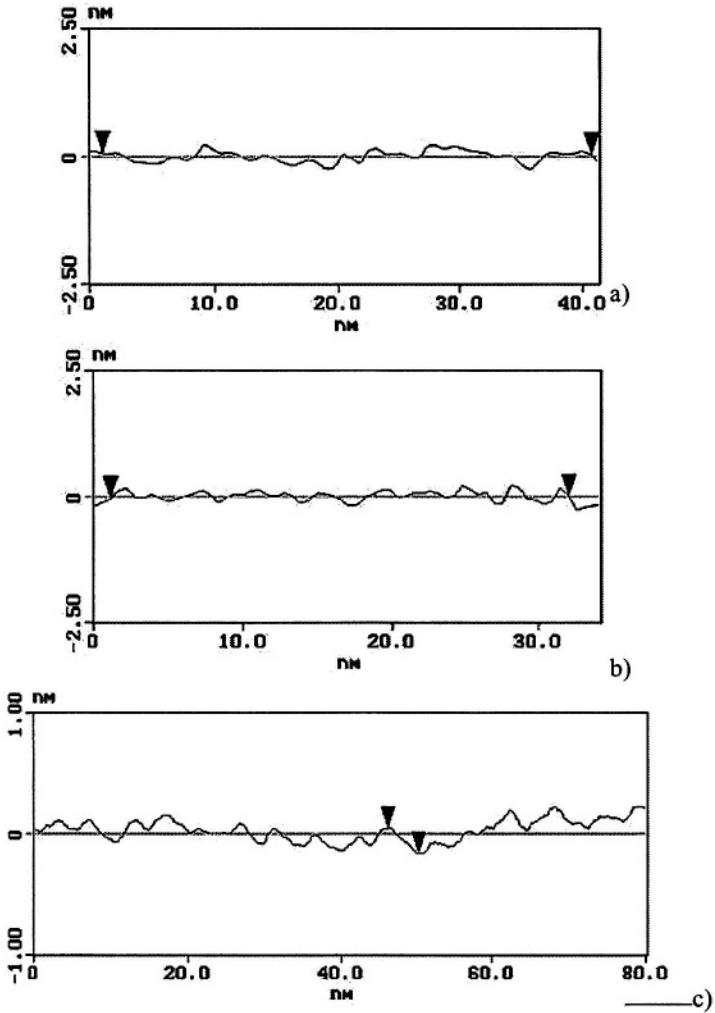


Figure 20. The line sections analysis of the flat parts of surfaces of the copper coatings electrodeposited from: a) *solution Cu I*,  $\delta = 20 \mu\text{m}$ ,<sup>15</sup> b) *solution Cu II*,  $\delta = 20 \mu\text{m}$ ,<sup>15</sup> c) *solution Cu I*,  $\delta = 25 \mu\text{m}$ ,<sup>13</sup> d) *solution Cu II*,  $\delta = 25 \mu\text{m}$ .<sup>12</sup> (Reprinted from Refs.<sup>12,13,15</sup> with permission from Elsevier and Springer-Verlag.)

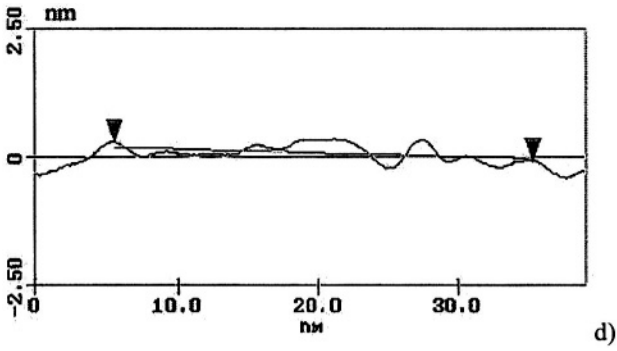


Figure 20. Continuation

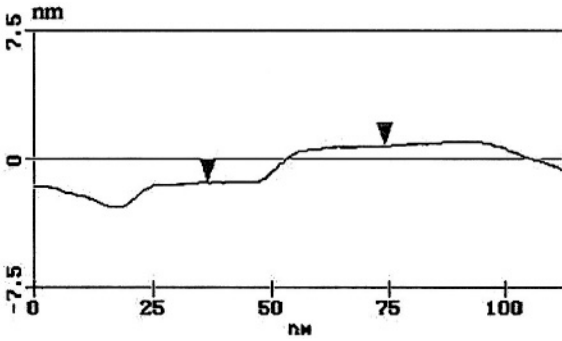


Figure 21. The line section analysis from a portion of  $40\ \mu\text{m}$  thick the copper coating electrodeposited from *solution Cu I*. (Reprinted from Ref. <sup>16</sup> with permission from Union of Engineers and Technicians for Protecting of Materials of Serbia.)

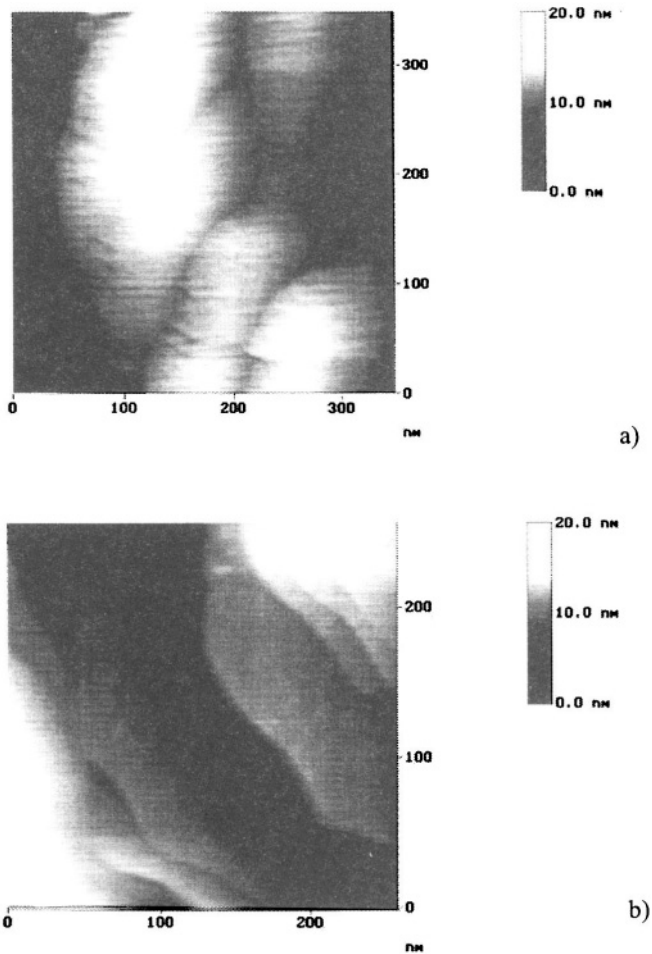


Figure 22. STM images of copper coatings electrodeposited from: a) *solution Cu I*,  $\delta = 20 \mu\text{m}$ ,<sup>15</sup> b) *solution Cu II*,  $\delta = 20 \mu\text{m}$ ,<sup>15</sup> c) *solution Cu I*,  $\delta = 25 \mu\text{m}$ ,<sup>13</sup> d) *solution Cu II*,  $\delta = 25 \mu\text{m}$ .<sup>17</sup> (Reprinted from Refs.<sup>13,15</sup> with permission from Elsevier and Springer-Verlag, respectively.)



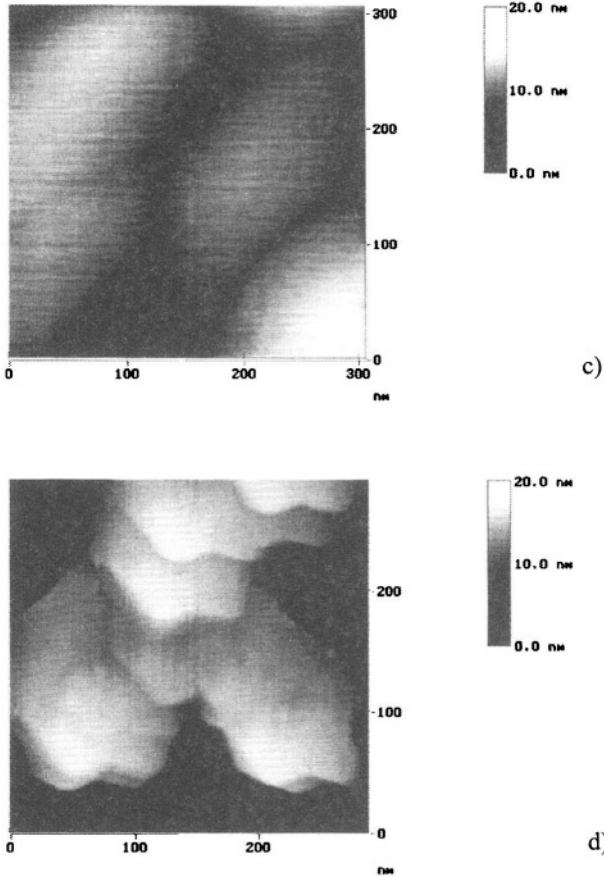


Figure 22. Continuation.

distances between adjacent flat parts were several atomic diameters of copper.<sup>11</sup> The flat parts of the surfaces were smooth on the atomic scale.

X-Ray diffraction (XRD) patterns of 20  $\mu\text{m}$  thick copper coatings obtained from *solution Cu I* and *solution Cu II* are shown in Figs. 23a and 23b, respectively. From Figs. 23a and 23b can be seen that the copper surfaces exhibited different preferred orientations. The copper coating electrodeposited from *solution Cu I* showed (111) preferred ori

**Table 1**  
**The Estimated Mean Sizes of Atomically Flat Parts of**  
**Copper Coatings**

STM	The estimated mean sizes of atomically flat parts of copper coatings electrodeposited from:			
	Cu I Solution		Cu II Solution	
	$\delta = 20 \mu\text{m}$ (160 x 200)	$\delta = 25 \mu\text{m}$ (140 x 240)	$\delta = 20 \mu\text{m}$ (140 x 160)	$\delta = 25 \mu\text{m}$ (160 x 170)
Functions:				
ACVF/ $\text{nm}^2$	229	243	166	198
PSD/ nm				

entation (Fig. 23a) while the copper coating obtained from *solution Cu II* showed (200) preferred orientation (Fig. 23b).

Finally, it can be concluded on the basis of structural analysis of these copper coatings that structural characteristics did not depend on thickness of the coatings or preferred orientations.

### (iii) Zinc Coatings

#### (a) Reflection analysis

The reflection characteristics for the zinc coatings,<sup>18</sup> having thicknesses of 20, 25 and 60  $\mu\text{m}$ , electrodeposited onto copper cathodes, obtained from the acid sulfate solution containing the dextrin/salicyl aldehyde mixture (*solution Zn I*: 300  $\text{g l}^{-1}$   $\text{ZnSO}_4 \cdot 7 \text{H}_2\text{O}$  + 30  $\text{g l}^{-1}$   $\text{Al}_2(\text{SO}_4)_3 \cdot 18 \text{H}_2\text{O}$  + 15  $\text{g l}^{-1}$   $\text{NaCl}$  + 30  $\text{g l}^{-1}$   $\text{H}_3\text{BO}_3$  + 3.0  $\text{g l}^{-1}$  dextrin + 2.8  $\text{ml l}^{-1}$  salicyl aldehyde), are shown in Fig. 24. The degree of mirror reflection reached 85 %, while the degree of diffuse reflection from these coatings is quite small (up to 5%). Also, it can be observed from this figure that the degree of mirror reflection increases with increasing thickness of the zinc coatings.

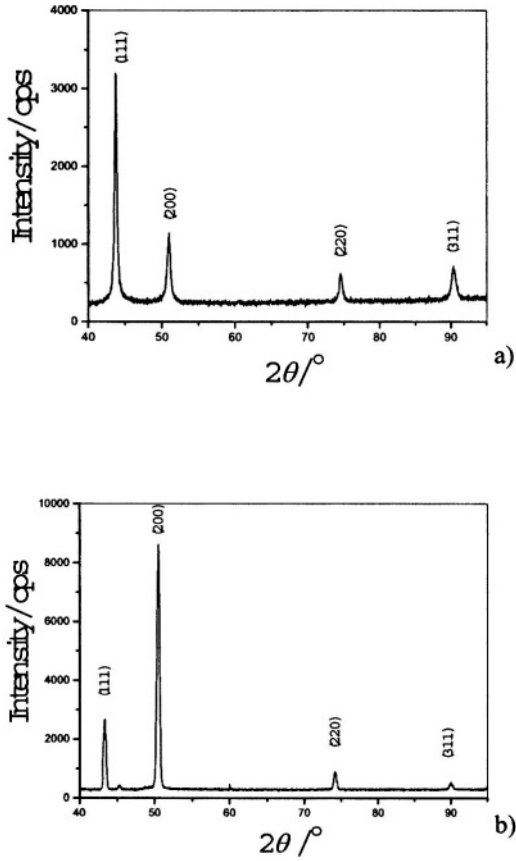


Figure 23. XRD patterns of  $20\ \mu\text{m}$  thick copper coatings electrodeposited from: a) solution Cu I, b) solution Cu II. (Reprinted from Ref. <sup>15</sup> with permission from Springer-Verlag.)

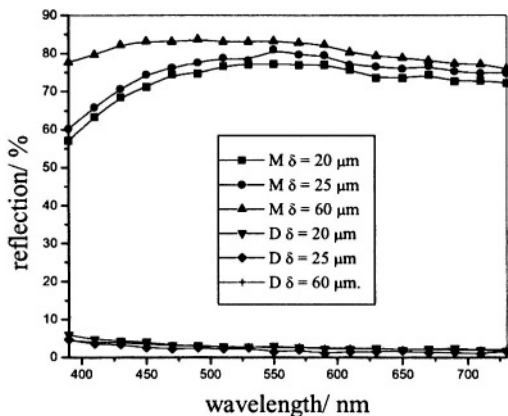


Figure 24. The dependence of the degree of reflection on the visible light wavelength for zinc coatings obtained from solution containing the dextrin/salicyl aldehyde mixture (*solution Zn I*). M: mirror reflection, D: diffuse reflection. (Reprinted from Ref.<sup>18</sup> with permission from the Serbian Chemical Society.)

### (b) Structural analysis

It can be seen from Fig. 25 that the zinc coating obtained from *solution Zn I* is relatively smooth, but without large flat and mutually parallel parts of the surface, which were characteristic of the previously observed copper surfaces (see Section II.2(i) and Section II.2(ii)). The surfaces of zinc coatings of thicknesses 20 and 60  $\mu\text{m}$  were very similar to that of the zinc coating of thickness 25  $\mu\text{m}$  and, consequently, the STM images of these zinc coatings are not presented.

Analysis of the zinc coatings at even higher magnification led to the morphologies shown in Fig.26, where the light tones represent high areas in the STM images. The analyzed surface was (50 x 50) nm. As can be seen from Fig. 26, surfaces of these zinc coatings are covered with hexagonal zinc crystals.

The line sections analysis of these later morphologies are shown in Fig. 27, from which it can be observed that the top surfaces of the hexagonal zinc crystals are relatively flat and mutually parallel.

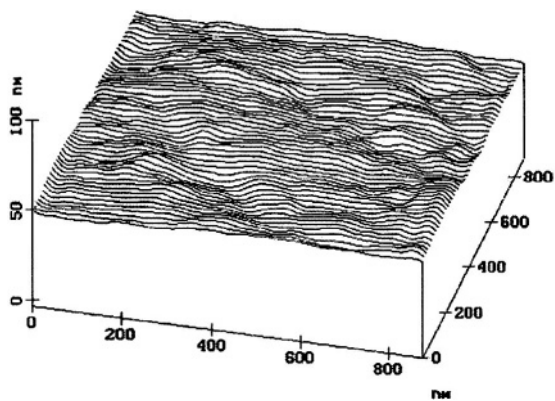
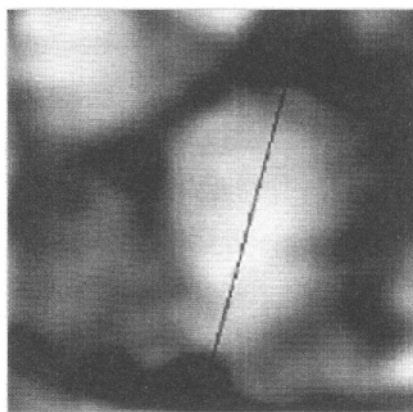


Figure 25. 3D STM image of the zinc coating obtained from *solution Zn I*. Scan size: (880 x 880) nm. (Reprinted from Ref.<sup>18</sup> with permission from the Serbian Chemical Society.)



a)

Figure 26. STM images of zinc coatings and the average roughness of the observed hexagonal zinc crystals: a)  $20\ \mu\text{m}$ ,  $R_a = 0.252\ \text{nm}$ , b)  $25\ \mu\text{m}$ ,  $R_a = 0.264\ \text{nm}$ , c)  $60\ \mu\text{m}$ ,  $R_a = 0.185\ \text{nm}$ . Scan size: (50 x 50) nm. (Reprinted from Ref.<sup>18</sup> with permission from the Serbian Chemical Society.)

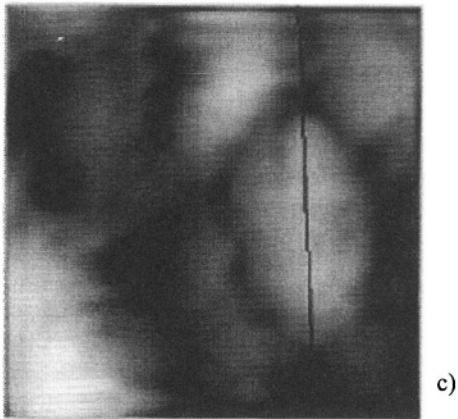
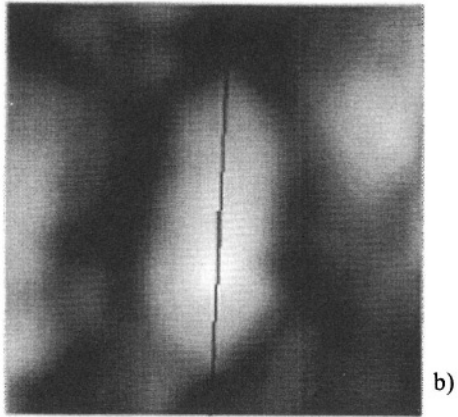


Figure 26. Continuation

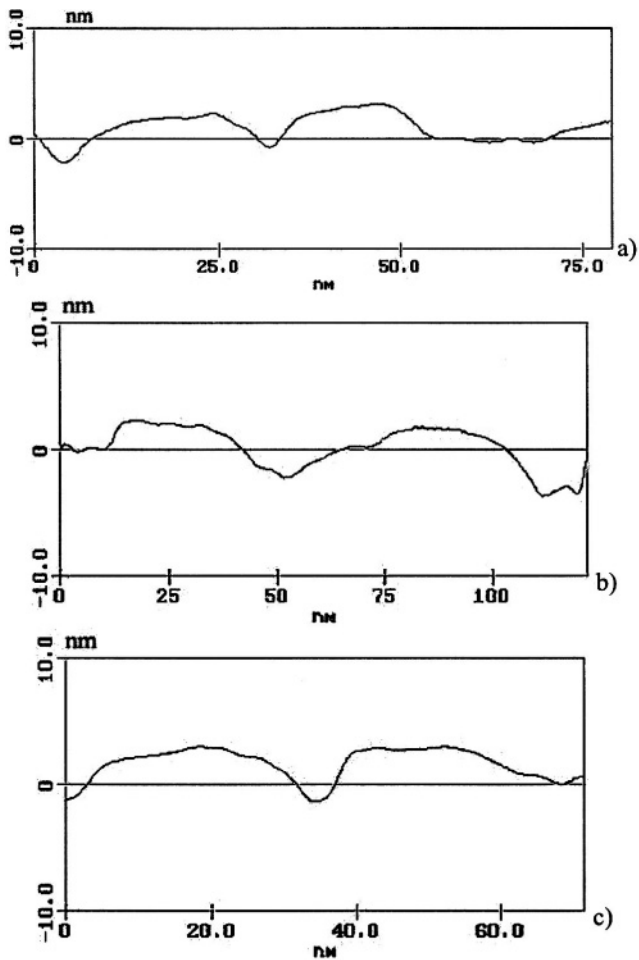


Figure 27. Typical surface profile of zinc coatings from (50 x 50) nm STM images: a) 20  $\mu\text{m}$ , b) 25  $\mu\text{m}$ , c) 60  $\mu\text{m}$ . (Reprinted from Ref.<sup>18</sup> with permission from the Serbian Chemical Society.)

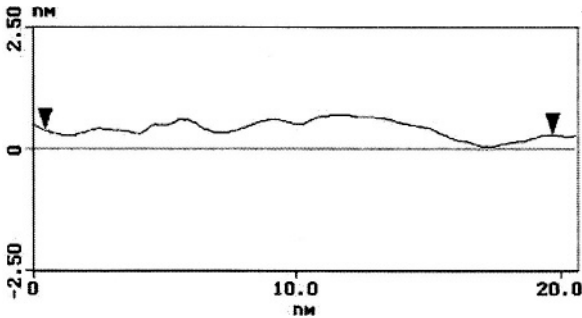


Figure 28. The line sections analysis a surface of hexagonal zinc crystal. (Reprinted from Ref.<sup>15</sup> with permission from Springer-Verlag.)

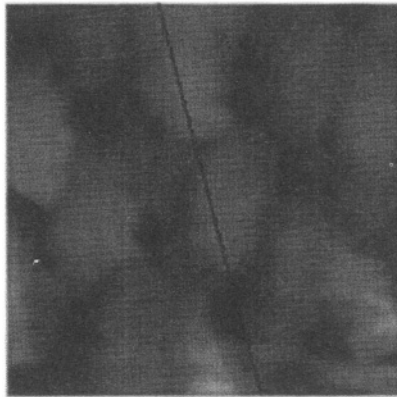


Figure 29. STM image of zinc coating obtained from *solution Zn I*; cathode: zinc. Scan size: (60 x 60) nm. (Reprinted from Ref.<sup>19</sup> with permission from Union of Engineers and Technicians for Protecting of Materials of Serbia.)

It is also shown by the STM software measurements that the roughness of the hexagonal zinc crystals from Fig. 28 is on the atomic level, *i.e.*, less than the atomic diameter of zinc.<sup>11</sup>

The mean size of this hexagonal zinc crystal (estimated by the STM software data processing) was by approximately (18 x 20) nm<sup>2</sup> by the ACVF and about 20 nm by the PSD functions.

Figures 29 and 30 show structural analysis of the 25 μm thick zinc coating electrodeposited in the presence of the same brightening



addition agents, but onto a zinc cathode.<sup>19</sup> The degrees of mirror and diffuse reflection of this coating were very close to the same degrees for the zinc coating electrodeposited onto a copper cathode. It can be seen from Fig. 29 that the surface of this zinc coating is again covered with hexagonal zinc crystals. From Fig. 30 it can be seen that the top planes of these zinc crystals are flat and mutually parallel. These zinc crystals exhibit a smoothness on the atomic scale.

Structural STM analysis of the zinc coating obtained from solution containing the dextrin/furfural mixture are shown in Figs. 31 and 32.<sup>13</sup> Reflection characteristics of zinc coating obtained from the *solution Zn II* (*solution Zn II: 300 g l<sup>-1</sup> ZnSO<sub>4</sub> · 7 H<sub>2</sub>O + 30 g l<sup>-1</sup> Al<sub>2</sub>(SO<sub>4</sub>)<sub>3</sub> · 18 H<sub>2</sub>O + 15 g l<sup>-1</sup> NaCl + 30 g l<sup>-1</sup> H<sub>3</sub>BO<sub>3</sub> + 3.0 g l<sup>-1</sup> dextrin + 1.4 ml l<sup>-1</sup> furfural*) were very close to reflection characteristics of the zinc coating obtained from solution containing the dextrin/salicyl aldehyde mixture. The surface of this zinc coating is relatively smooth (Fig. 31), covered by zinc crystals, the top planes of which are flat and mutually parallel (Fig. 32). These zinc crystals were smooth on the atomic scale. The estimated mean size of these atomically flat zinc crystals was approximately (30 x 40) nm<sup>2</sup> according to the ACVF function and approximately 31.35 nm by the PSD function.<sup>13</sup>

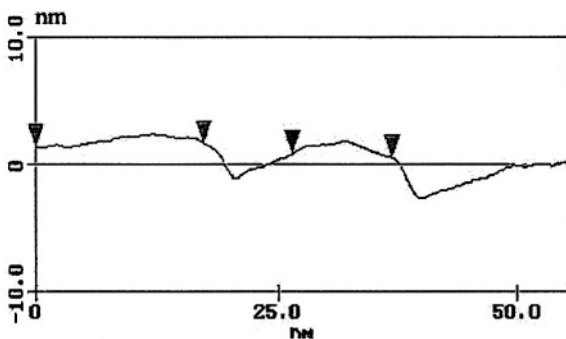


Figure 30. The line section analysis from the portion of the STM surface shown in Fig. 21. (Reprinted from Ref.<sup>19</sup> with permission from Union of Engineers and Technicians for Protecting of Materials of Serbia.)

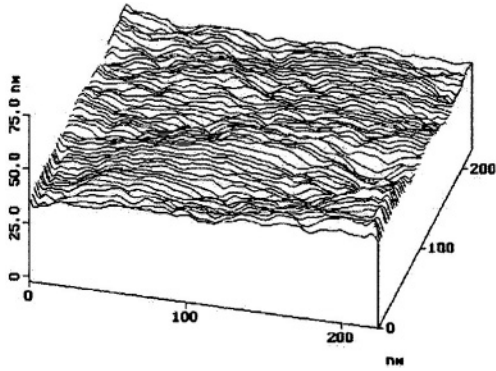


Figure 31. STM image of zinc coating obtained from solution containing the dextrin/furfural mixture (*solution Zn II*). Scan size: (300 x 300) nm. (Reprinted from Ref.<sup>13</sup> with permission from Elsevier.)

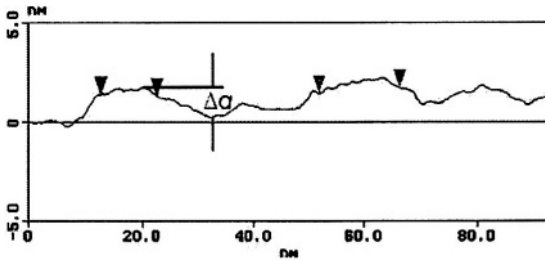


Figure 32. The line section analysis from the portion of the STM surfaces shown in Fig. 31. The vertical distance:  $\Delta a = 1.379$  nm. (Reprinted from Ref.<sup>13</sup> with permission from Elsevier.)

*(iv) Nickel Coatings**(a) Reflection analysis*

The ideal reflectance of nickel<sup>10</sup> and the degrees of total reflection as a function of wavelength of visible light for a nickel coating electrodeposited in the presence of the basic brightening addition agent and the nickel coating electrodeposited in the presence of both the basic and the top brightening addition agents<sup>20</sup> are shown in Fig. 33a. The degrees of mirror and diffuse reflections of the same nickel coatings as a function of wavelength are shown in Fig. 33b.

It can be seen from Fig. 33b that the addition of the top brightening addition agent to a nickel plating bath containing the basic brightening additive led to an increase of the degree of mirror reflection and a decrease of the degree of diffuse reflection. The degree of mirror reflection of the nickel coating obtained in the coating obtained in the presence of the basic brightening addition agent only. Also, it can be observed from Fig. 33 that the degree of mirror reflection of the nickel coating obtained in the presence of the basic and top-brightening-addition agents approaches very nearly the ideal reflectance of nickel. Although the degree of mirror reflection of the nickel coating, obtained in the presence of the basic and top brightening addition agents, was only 3 - 6 % greater and the degree of diffuse reflection was only 4 % smaller than the same degrees of the nickel coating obtained in the presence of the basic brightening addition agent alone, a visual difference between these nickel coatings was apparent.

*(b) Structural analysis*

The addition of the top brightening addition agent to the plating bath containing only the basic brightening addition agent led to a decrease of the roughness of the nickel coating, as illustrated by Fig. 34.

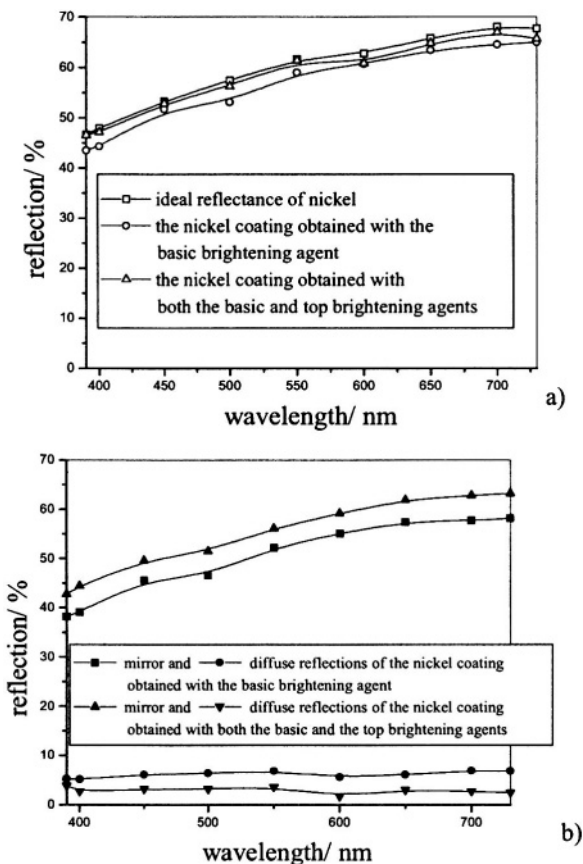


Figure 33. The dependence of the degrees of reflection on the wavelength of visible light: a) the ideal reflectance of nickel (□) and the total reflections of the nickel coating electrodeposited in the presence of the basic brightening addition agent (○) and the nickel coating electrodeposited in the presence of both the basic and the top brightening addition agents (△); b) mirror (■) and diffuse (●) reflections of the nickel coating electrodeposited in the presence of the basic brightening addition agent alone; mirror (▲) and diffuse (▼) reflections of the nickel coating electrodeposited in the presence of both the basic and the top brightening addition agents.<sup>20</sup> (Reprinted from Ref.<sup>20</sup> with permission from the Serbian Chemical Society.)

Relatively flat parts of the surface can be observed both for the nickel coating obtained in the presence of the basic brightening addition agent only and the nickel coating obtained in the presence of both the basic and top brightening addition agents (Fig. 35). From Fig.

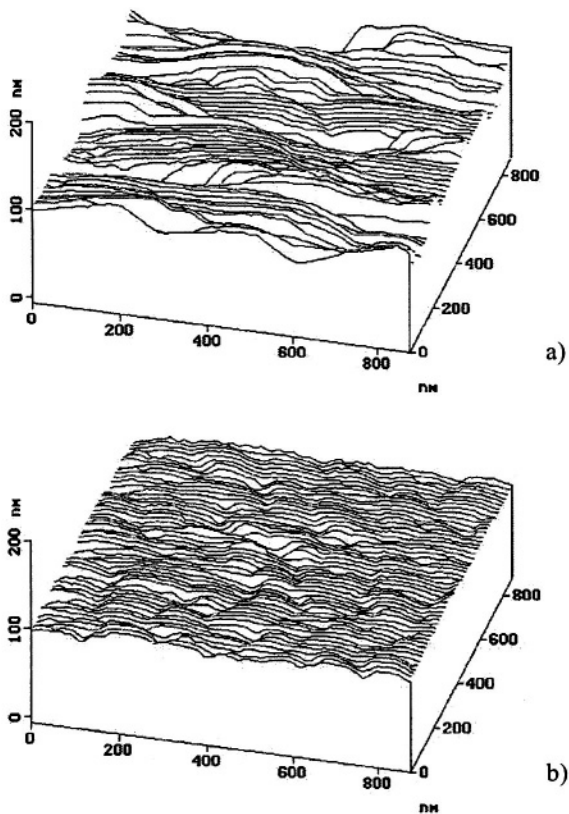


Figure 34. 3D STM images of the nickel coatings electrodeposited with: a) basic brightening addition agent, b) both basic and top brightening addition agents. Scan size: (880 x 880) nm. (Reprinted from Ref.<sup>20</sup> with permission from the Serbian Chemical Society.)

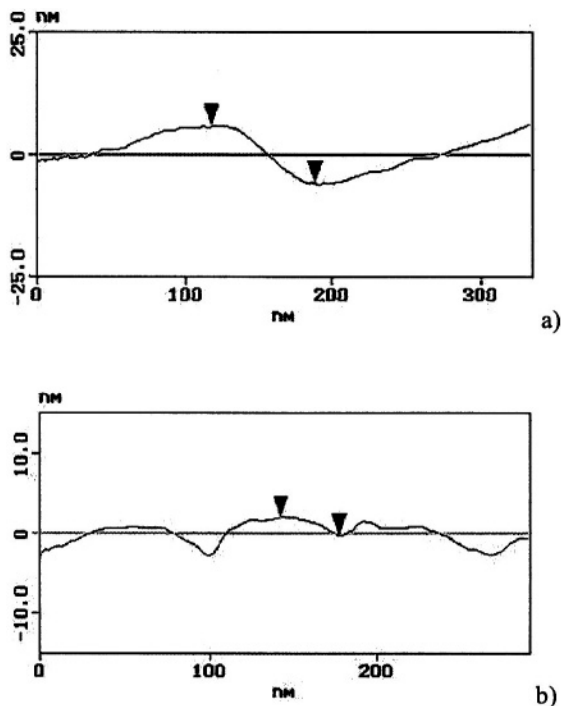


Figure 35. The line sections analysis from the portion of the STM surfaces shown in Fig. 34: a) the nickel coating obtained in the presence of the basic brightening addition agent, b) the nickel coating obtained in the presence of both the basic and the top brightening addition agents. The distances between the markers represent: a) 11.650 nm; b) 2.335 nm. (Reprinted from ref. 20 with permission from the Serbian Chemical Society.)

35b it can be seen that the nickel coating obtained in the presence of both the basic and top brightening addition agents consisted of flat and mutually parallel parts of the surface. It was shown by the STM software that the distances between adjacent flat parts of the nickel coating obtained in the presence of the basic brightening addition agent only are several times greater than the same distances of the nickel coating obtained in the presence of both the basic and the top

brightening addition agents. The distance between adjacent flat parts of the nickel coating obtained in the presence of both the basic and the top brightening addition agents is several atomic diameters of nickel.<sup>11</sup> The same distance for the nickel coating obtained in the presence of the basic brightening addition agent only is approximately 40 atomic diameters of nickel.

The line section analysis of the flat part of the nickel coating obtained in the presence of both the basic and the top brightening addition agents is shown in Fig. 36. The roughness of this flat part of the surface is very small and less than the atomic diameter of nickel. For this reason, it can be said that the flat parts of the surface are smooth on the atomic level.

*(v) Discussion of presented results and the model*

On the basis of reflection and structural analyses of the silver mirror and other different metal surfaces, it can be concluded that the light from flat parts of surface is mirror reflected light. The diffuse reflection arises from the parts of the surface between the flat parts of surface. Hence, these parts of a surface scatter light.

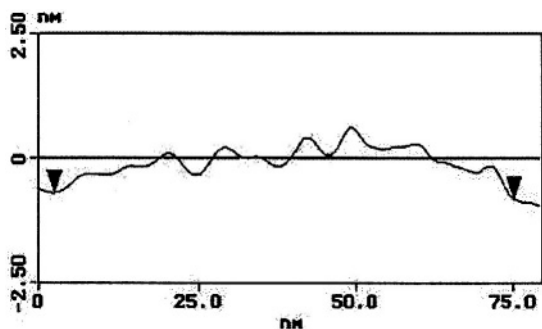


Figure 36. The line section analysis of the flat part of the nickel coating obtained in the presence of both the basic and the top brightening addition agents. The roughness of the observed surface was 0.220 nm. (Reprinted from Ref.<sup>20</sup> with permission from the Serbian Chemical Society.)

Reflection analysis of a silver mirror surface taken as a reference standard showed that the reflection of light from this surface is mostly mirror reflection and that the degrees of mirror reflection are very close to the ideal reflectance of silver. The structural characteristics of this surface, which provide a high degree of mirror reflection, are flat and mutually parallel parts which are smooth on the atomic level, with adjacent flat parts being separated by several atomic diameters of silver.

Hence, the conditions which must be fulfilled in order for metal surfaces to be mirror bright are: (i) flat parts of the surface which are smooth on the atomic level and (ii) distances between adjacent flat parts are comparable with the distances between the adjacent flat parts of a silver mirror.

Similarity of structural characteristics were shown by the the copper surface polished both mechanically and electrochemically, the copper coatings obtained from *solutions Cu I* and *Cu II*, the zinc coatings obtained from *solutions Zn I* and *Zn II* and the nickel coating obtained in the presence of both the basic and the top brightening addition agents (see 2.2.1–2.2.4). For that reason, these metal surfaces can be classified as mirror bright. On the other hand, the copper coating polished mechanically only and the nickel coating obtained in the presence of the basic brightening addition agent only, can be considered as semi-bright metal surfaces.

The variety of results presented can be illustrated by a simple model which treats brightness from the point of view of geometrical optics only.<sup>12</sup> The proposed model will be valid if the following assumptions are fulfilled:

- Metal surfaces are divided into equal elementary parts for which the surface area is  $n$ ;
- the flat parts are smooth;
- the light falls onto the surface at a determined angle, and is reflected from the surface only in the direction making an angle with the normal equal to the angle of incidence;
- *the upper flat parts of a surface area ( $k_u n$  parts) reflect light completely; and*
- *the parts of the lower flat parts of a surface area ( $k_l n$  parts) do not reflect light completely because they are screened by the height of the lateral parts of a surface area ( $k_l n$  parts). The screened zones are made by both incident and reflected lights.*



In total, the brightness of a surface is determined by the ratio of flat parts to the surface between adjacent flat parts. Increasing the distance between adjacent flat parts leads to a decreasing brightness of the surface.<sup>12</sup>

The parts of the surface which are not able to reflect light,  $e_i$ , depend on the angle of incidence angle and the height of the lateral part of the surface. The effect of these factors is illustrated in Figs. 37a, 37b and 37c show that there is an additivity of the parts of the surface which are not

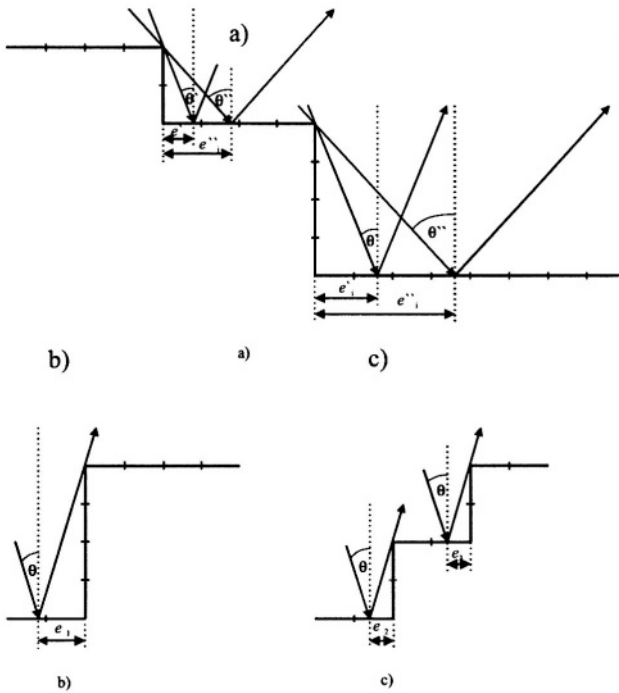


Figure 37. Schematic representation of line section showing the effects of different factors on the reflection of light from a surface: a) the angle of incidence  $\theta$  and the height of a lateral part of a surface, b) and c) additivity of the parts of a surface which do not have the ability to reflect light. (Reprinted from Ref.<sup>12</sup> with permission from Elsevier.)

able to reflect light, *i.e.*, the screened part of the surface shown in Fig. 37b (denoted as  $e_1$ ) is equal to the sum of screened parts of the surface shown in Fig. 37c (denoted as  $e_2$  and  $e_3$ ). Hence,

$$e = \sum_1^{\infty} e_i \quad (1)$$

where  $i = 0, 1, 2, 3, \dots$

Then, mirror bright surfaces can be simulated by Fig. 38a, semibright surfaces by Fig. 38b and a surface which would show a small degree of mirror reflection (*i.e.*, a metal coating obtained from a solution in the absence of brightening addition agents) by Fig. 38c (see Figs. 8a, 11, 19, 21, 27, 30, 32 and 35).

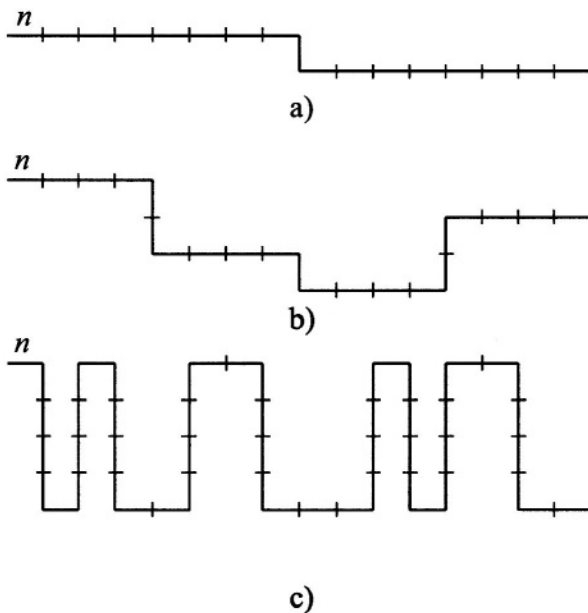


Figure 38. Schematic presentation of the different metal surfaces: a) mirror bright metal surfaces, b) semi-bright metal surfaces, c) a surface which would show a small degree of mirror reflection. (Reprinted from Ref.<sup>12</sup> with permission from Elsevier.)

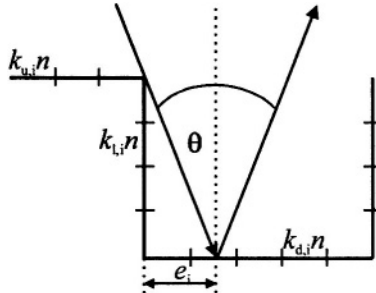


Figure 39. Line-section simulation of one surface of unit a metal surface.

These metal surfaces can be represented by one equivalent surface which consists of row elementary surface units. One such surface unit is represented in Fig. 39.

It can be shown by simple mathematics that the part of the surface which is screened,  $e_i$ , and so cannot reflect light is given, for an angle of incidence,  $\theta$ , by Eq. (2),

$$e_i = k_{l,i} \cdot n \cdot \text{tg}\theta \tag{2}$$

where  $i = 0, 1, 2, 3, \dots$

Then, having in mind fact that the screened zones are made by both incident and reflected lights, the brightness of a surface, defined as the ratio of the geometrical minus the screened surface and the geometrical surface, can be given by Eq. (3):

$$\text{brightness} = \frac{\sum_1^{\infty} k_{u,i} \cdot n + \left( \sum_1^{\infty} k_{d,i} \cdot n - 2 \sum_1^{\infty} e_i \right)}{\sum_1^{\infty} k_{u,i} \cdot n + \sum_1^{\infty} k_{d,i} \cdot n} \tag{3}$$

$$\begin{aligned}
 &= \frac{k_u \cdot n + (k_d \cdot n - 2 \cdot e)}{k_u \cdot n + k_d \cdot n} = \frac{k_u \cdot n + \left( k_d \cdot n - 2 \cdot \sum_1^{\infty} k_{l,i} \cdot n \cdot \operatorname{tg} \theta \right)}{k_u \cdot n + k_d \cdot n} \\
 &= \frac{k_u + (k_d - 2k_l \operatorname{tg} \theta)}{k_u + k_d} = 1 - 2 \frac{k_l}{k_u + k_d} \operatorname{tg} \theta
 \end{aligned}$$

where

$$k_u = \sum_1^{\infty} k_{u,i}, \quad k_d = \sum_1^{\infty} k_{d,i}, \quad k_l = \sum_1^{\infty} k_{l,i} \quad (4)$$

Hence, according to Eq. (3), the brightness of a surface is a function of the incident angle  $\theta$ , and the ratio between the flat parts,  $(k_u + k_d)$  and the lateral parts,  $k_l$ . Increasing the lateral parts of a surface,  $k_l$  leads to a decrease in the brightness of the surface. Therefore, when  $k_l \rightarrow 0$ , then the brightness of the surface approaches that of a mirror.

The boundary conditions of Eq. (3) depend on the expression in the bracket in the following way:

$$k_{d,i} - 2k_{l,i} \operatorname{tg} \theta = \begin{cases} k_{d,i} - 2k_{l,i} \operatorname{tg} \theta & \operatorname{tg} \theta < \frac{k_{d,i}}{2k_{l,i}} & (4a) \\ 0 & \operatorname{tg} \theta \geq \frac{k_{d,i}}{2k_{l,i}} & (4b) \end{cases}$$

Hence, *the lower flat parts of a surface area will reflect light only if the condition (4a) is fulfilled, i.e., if tangent of an incident angle of light is smaller than the ratio  $(k_{d,i}/2 k_{l,i})$ . On the other hand, for larger incident angles or an incident angle equal to this ratio, the lower flat parts of a surface area will not be able to reflect light (the condition given by Eq. 4b).*

Then, the consequences will be:

$$\theta = 0 \quad \text{brightness} = 1 \quad (4.c)$$

and

$$\text{tg}\theta \geq \frac{k_{d,i}}{2k_{l,i}} \quad \text{brightness} = \frac{k_u}{k_u + k_d} \quad (4d)$$

This means that the brightness of a surface decreases from 1 to some value given by Eq. (4d) with increase of the angle of incident light from 0 to some critical value.

It is necessary to note that an increase of the lateral parts of a surface,  $k_l$  is accompanied by an increase of the “degree of development of the surface.” The later quantity,  $S'$ , defined as the ratio of the real (actual) to geometrical surface, is given by Eq. (5):

$$S' = \frac{k_u \cdot n + k_d \cdot n + 2k_l \cdot n}{k_u \cdot n + k_d \cdot n} = 1 + 2 \frac{k_l}{k_u + k_d} \quad (5)$$

Then, according to Eqs. (3) and (5), the brightness of a surface can be defined by Eq. (5),

$$\text{brightness} = 1 - S \text{tg} \theta \quad (6a)$$

or, in %, by Eq. (6a)

$$\text{brightness (in \%)} = 100 - S \text{ (in \%)} \cdot \text{tg}\theta \quad (6b)$$

where  $S = (S' - 1)$  – a quantity experimentally measurably by STM data processing as *the surface area diff.*

The degrees of development of a surface, determined by the STM analysis as *the surface area diff.*, for the silver mirror surface, the copper surface polished mechanically only and the mirror-bright copper coating obtained from *solution Cu II* of 25  $\mu\text{m}$  thickness, calculated from an area (880 x 880)  $\text{nm}^2$ , are given in Table 2.<sup>12</sup>

The results presented and the model can be verified in the following way. According to this model, the brightness of a surface depends on the angle of incidence and the ratio between the flat, ( $k_u + k_d$ ) and the lateral parts,  $k_l$ .

**Table 2**  
**The Values *The Surface Area Diff* (*S*, %) for Copper Surfaces**  
**from an (880 x 880) nm<sup>2</sup> area. (Reprinted from Ref.<sup>12</sup> with**  
**permission from Elsevier.)**

Surface area diff.	Silver mirror surface	Copper surface polished mechanically	The mirror bright copper coating obtained from solution Cu II of 25 μm thickness
S, %	3.2 ± 0.2	94.0 ± 3.0	4.1 ± 0.3

The effect of the incident angle of light is illustrated by the results of the measurements of the mirror-reflected light from copper surfaces which were illuminated at 5° and 30° with respect to the normal to the surface. It should be noted that these results cannot be compared directly with the ones from Figs. 1, 6, 9, 15, 16, 24 and 33. Table 3 gives the values of the amount of mirror reflected light, in %, with respect to a mirror as the reference standard, from the copper coating obtained from *solution Cu II* of 25 μm thickness and the copper surface polished only mechanically. A value of 100 % means that the reflection of light approaches that from a mirror. Smaller values of the amount of mirror reflected light correspond to a decrease of the reflection of light with respect to that from a mirror.

**Table 3**  
**The Amount of Mirror-Reflected Light and Brightness of**  
**Surface Determined According to Eq. (6b). (Reprinted**  
**from Ref.<sup>12</sup> with permission from Elsevier.)**

Surface	The amount of mirror reflected light, in %, for incident angles		Brightness calculated according to Eq. (6b), in %, for incident angles	
	5°	30°	5°	30°
Silver mirror	100	100	99.72	98.15
Coating obtained from <i>solution Cu II</i> of 25 μm thickness	100	91.2	99.64	97.63
Surface polished mechanically	88.9	51.5	91.78	45.73

It can be seen from Table 3 that increasing the angle of incidence leads to a decrease of the degree of specular reflection of a surface. The reflection of light from the copper coating obtained from *solution Cu II* of  $25 \mu\text{m}$  thickness approaches that from a mirror. On the other hand, the reflection of light from the copper surface polished only mechanically is smaller than that from a mirror and the difference in the light reflection increases strongly with increasing incident angle.

Brightness of copper and silver mirror surfaces, calculated according to Eq. (6b), using values of degrees of development of surfaces determined by STM data processing (Table 2) and the degree of development of the silver mirror surface, for the same incident angles are given in Table 3. Table 3 shows that there is agreement within the limits of the experimental error, between experimentally obtained values of mirror reflected light and those of brightness obtained according to the proposed model (Eq. 6b).

The effect of the ratio between the flat and lateral parts can be verified easily by comparative analysis of reflection and structural characteristics of metal surfaces that were considered in Sections II.1 and II.2. Increasing the ratio of flat to lateral parts of surface areas from values corresponding to mat surfaces to those of metal surfaces denoted as mirror bright lead to increasing degrees of mirror reflection, *i.e.*, the reflection of light approaches that of a mirror. This obviously cannot be estimated from measurements of reflection at low light incident angle, because as  $\theta \rightarrow 0$  the role of the lateral parts of surfaces becomes negligible. Hence, in order to define a metal surface as mirror bright by measurements of reflection, it is necessary to perform the determination of reflection at  $\theta = 0$  in order to determine the quality of the flat parts of surfaces and at least at one relatively large angle (as, for example,  $30^\circ$ ) in order to determine the role of the lateral parts in light reflection. Hence, if reflection at both incident angles (0 and, for example,  $30^\circ$ ) approaches that of a mirror at the same incident angles, the surface can be denoted as mirror bright. Hence, these results represent a good semi-quantitative affirmation of the proposed mathematical model.

Also, the brightness of a metal surface depends on the mean size of atomically flat parts. The difference in the maximum degrees of mirror reflection between the copper coatings (above 85 %) and the zinc coatings (below 85 %) can be ascribed to the different mean size of atomically flat parts of the copper and zinc coatings (see Figs. 22 and 29). The smaller mean size of atomically flat parts of a surface, the greater is the ratio of screened parts which do not have the ability to

reflect light. In both cases, the distances between adjacent flat parts are approximately same, and comparable with the same distances between adjacent flat parts of a silver mirror surface.<sup>15</sup>

Finally, the different preferred orientations of copper coatings, as well as the copper surface polished both mechanically and electrochemically, which are characterized as mirror bright metal surfaces, clearly indicate that mirror brightness of a surface is not associated with a preferred orientation. Also, the preferred orientations of the copper coatings did not depend on type of electrodes used.<sup>21</sup>

The properties which determine whether the metal surface is mirror bright are precisely determined by STM investigations. It is also shown that mirror bright metal surfaces can be obtained only by electrochemical polishing or electrochemical deposition in the presence of brightening addition agents. Hence, the next step in investigations of bright metal surfaces should be the determination of the mechanisms by which they are formed during corresponding electrochemical processes. For example, the mechanism of formation of bright copper surfaces can probably be easily done by correlating the results of Nichols and coworkers<sup>5</sup> on the structure of the copper surfaces obtained in the presence of additives, with their reflection characteristics.

### ACKNOWLEDGMENTS

This work was supported by the Ministry of Sciences, Technologies and Development of the Republic of Serbia under the research projects "Electrodeposition of Metal Powders at a Constant and at a Periodically Changing Rate" 1806/2002) and "Surface Science and Thin Films" (2018/2002).

### REFERENCES

- <sup>1</sup> J.O'M. Bockris, G. A. Razumney, "Fundamental Aspects of Electrocrystallization", Plenum Press, New York, 1967.
- <sup>2</sup> R. Weil, R. A. Paquin, *J. Electrochem. Soc.*, **107** (1960) 87.
- <sup>3</sup> J.K. Dennis, T.E. Such, Nickel and Chromium plating, Woodhead Publ. Ltd, Cambridge England, 1993.
- <sup>4</sup> R. Weil, H. C. Cook, *J. Electrochem. Soc.*, **109** (1962) 295.



- <sup>5</sup> R. J. Nichols, C. E. Bach, H. Meyer, *Ber. Bunsenges. Phys. Chem.*, **97** (1993) 1012.
- <sup>6</sup> F. Czerwinski, K. Kondo, J. A. Szpunar, *J. Electrochem. Soc.*, **144** (1997) 481.
- <sup>7</sup> N.D.Nikolić, Z.Rakočević, K.I.Popov, *J. Serb. Chem. Soc.*, **66** (2001) 723.
- <sup>8</sup> N.D.Nikolić, Z.Rakočević, K.I.Popov, *Materials Protection*, **42** (2001) 25 (in Serbian).
- <sup>9</sup> N.D.Nikolić, E.R.Stojilković, K.I.Popov, M.G.Pavlović, *J. Serb. Chem. Soc.*, **63** (1998) 877.
- <sup>10</sup> A.D.Rakić, A.B.Djuričić, J.M.Elazar, M.L.Majewski, *Applied Optics*, **37**(1998)5271.
- <sup>11</sup> D. Grdenić, Molekule i kristali, Školska knjiga, Zagreb, 1987 (in Croatian).
- <sup>12</sup> N. D. Nikolić, Z. Rakočević, K. I. Popov, *J.Electroanal.Chem.* **514** (2001) 56.
- <sup>13</sup> N.D. Nikolić, G. Novaković, Z. Rakočević, D. R. Đurović, K. I. Popov, *Surface and Coating Technology*, **161** (2002)188.
- <sup>14</sup> K. I. Popov, M. G. Pavlović, Z. Rakočević, and D. Škorić, *J. Serb. Chem. Soc.*, **60** (1995) 873.
- <sup>15</sup> N. D. Nikolić, Z. Rakočević, K. I. Popov, *J. Solid State Electrochemistry*, submitted for publication.
- <sup>16</sup> N. D.Nikolić, G. Novaković, Z. Rakočević, K. I. Popov, *Materials Protection*, **44** (2003)17 (in Serbian).
- <sup>17</sup> N. D. Nikolić, B. Starčević, Z. Rakočević, K. I. Popov, unpublished data.
- <sup>18</sup> N. D. Nikolić, K. I. Popov, Z. Rakočević, D. R. Đurović, M. G. Pavlović, and M. Stojanović, *J. Serb. Chem. Soc.* **65** (2000) 819.
- <sup>19</sup> N. D. Nikolić, K. I. Popov, Z. Rakočević, M. G. Pavlović, M. Stojanović, *Materials Protection*, **41** (2000) 27 (in Serbian).
- <sup>20</sup> N. D. Nikolić, Z. Rakočević, D. R. Đurović, K. I. Popov, *J. Serb. Chem. Soc.*, **67** (2002) 437.
- <sup>21</sup> N. D. Nikolić, E. R. Stojilković, D. R. Đurović, M.G. Pavlović, V. R. Knežević, *Materials Science Forum*, **352** (2000) 73.